Neurobiology of Stress 8 (2018) 10–20

Contents lists available at ScienceDirect

Neurobiology of Stress

journal homepage: www.elsevier.com/locate/ynstr

Differential impact of *Met* receptor gene interaction with early-life stress on neuronal morphology and behavior in mice

Hanke Heun-Johnson[a], Pat Levitt[b,c,*]

[a] Neuroscience Graduate Program, University of Southern California, Los Angeles, CA, USA
[b] Institute for the Developing Mind, Children's Hospital Los Angeles, Los Angeles, CA, USA
[c] Department of Pediatrics, Keck School of Medicine, University of Southern California, Los Angeles, CA, USA

ARTICLE INFO

Keywords:
Early-life stress
Gene × environment interaction
MET receptor tyrosine kinase
Social-emotional behavior
Neuronal morphology

ABSTRACT

Early adversity in childhood increases the risk of anxiety, mood, and post-traumatic stress disorders in adulthood, and specific gene-by-environment interactions may increase risk further. A common functional variant in the promoter region of the gene encoding the human MET receptor tyrosine kinase (rs1858830 '*C*' allele) reduces expression of *MET* and is associated with altered cortical circuit function and structural connectivity. Mice with reduced *Met* expression exhibit changes in anxiety-like and conditioned fear behavior, precocious synaptic maturation in the hippocampus, and reduced neuronal arbor complexity and synaptogenesis. These phenotypes also can be produced independently by early adversity in wild-type mice. The present study addresses the outcome of combining early-life stress and genetic influences that alter timing of maturation on enduring functional and structural phenotypes. Using a model of reduced *Met* expression ($Met^{+/-}$) and early-life stress from postnatal day 2–9, social, anxiety-like, and contextual fear behaviors in later life were measured. Mice that experienced early-life stress exhibited impairments in social interaction, whereas alterations in anxiety-like behavior and fear learning were driven by *Met* haploinsufficiency, independent of rearing condition. Early-life stress or reduced *Met* expression decreased arbor complexity of ventral hippocampal CA1 pyramidal neurons projecting to basolateral amygdala. Paradoxically, arbor complexity in $Met^{+/-}$ mice was increased following early-life stress, and thus not different from arbors in wild-type mice raised in control conditions. The changes in dendritic morphology are consistent with the hypothesis that the physiological state of maturation of CA1 neurons in $Met^{+/-}$ mice influences their responsiveness to early-life stress. The dissociation of behavioral and structural changes suggests that there may be phenotype-specific sensitivities to early-life stress.

1. Introduction

Early-life adversity during childhood is associated with increased risk of anxiety, mood and post-traumatic stress disorders in adulthood (Green et al., 2010; Lang et al., 2008; Widom, 1999). Additionally, family and twin studies show that the heritability of these disorders is approximately 0.3–0.4 (Hettema et al., 2001; Stein et al., 2002; Sullivan et al., 2000). Genome-wide association studies and rare variant and mutation analyses have revealed several genetic risk factors associated with e.g. post-traumatic stress disorder (Almli et al., 2014), but a large fraction of heritability of many mental health disorders is still unexplained by single factors. Epidemiological studies have revealed gene-by-environment (G × E) interactions between early adversity, genetic polymorphisms, and increased risk for affective disorders (Bradley et al., 2008; Duncan et al., 2014; Sharma et al., 2015), but there is a need to discover G × E interactions that identify potential mechanisms of action.

In many early-life stress (ELS) rodent models, early adversity is induced by the disruption of postnatal maternal-pup interactions (Baram et al., 2012; Francis and Meaney, 1999; Heun-Johnson and Levitt, 2016; Raineki et al., 2010), which modulates long-term effects on behavior. ELS generally results in reduced social interactions and impaired fear memory in adult mice (Sachs et al., 2013; van der Kooij et al., 2015; Wang et al., 2011a), whereas reported effects on anxiety-like behaviors are mixed, with increased (Bouet et al., 2011; Levine et al., 2012; Mehta and Schmauss, 2011), decreased (Fabricius et al., 2008; Savignac et al., 2011) or unaffected outcomes (Ivy et al., 2008; Naninck et al., 2015; Sachs et al., 2013; Veenema et al., 2007; Zoicas

Abbreviations: ASD, autism spectrum disorders; BLA, basolateral amygdala; vHC, ventral hippocampus; DSI, direct social interaction; ELS, early-life stress; EPM, elevated-plus maze; G × E, gene-by-environment; P, postnatal day; SNP, single nucleotide polymorphism

* Corresponding author. The Saban Research Institute, Children's Hospital Los Angeles, 4650 Sunset Blvd. Mail stop #135, Los Angeles, CA 90027, USA.
E-mail address: plevitt@med.usc.edu (P. Levitt).

https://doi.org/10.1016/j.ynstr.2017.11.003
Received 1 August 2017; Received in revised form 24 November 2017; Accepted 25 November 2017
Available online 26 November 2017

and Neumann, 2016).

The social-emotional behaviors relevant to clinical manifestations associated with early life adversity in humans are regulated by specific neuronal activity in several brain regions in rodents, including the ventral hippocampus (vHC) and amygdala. These two structures are directly and reciprocally connected with each other (McDonald and Mott, 2017). Different experimental strategies have been used to stimulate, inhibit or record directly from CA1 neurons in different behavioral tasks, revealing the central role that vHC CA1 pyramidal neurons play in fear memory, anxiety-like behavior, spatial exploration, and goal-directed navigation (Ciocchi et al., 2015; Maren et al., 1998; Maren and Fanselow, 1995; Okuyama et al., 2016; Padilla-Coreano et al., 2016; Xu et al., 2016). Conversely, neurons projecting *from* the basolateral amygdala (BLA) to the vHC CA1 are involved in various social and emotional behaviors (Felix-Ortiz et al., 2013; Felix-Ortiz and Tye, 2014; Huff et al., 2016). These studies suggest that connectivity between the vHC and BLA, within larger networks of other brain regions, modulates behaviors integral to the effects of early adversity. Concomitantly, morphological changes may be apparent in neurons within this pathway after induction of ELS in mice. Indeed, ELS induces long-term morphological changes in amygdalar and (ventral) hippocampal neurons in mice and rats (Brunson et al., 2005; Ivy et al., 2010; Koe et al., 2016; Monroy et al., 2010), but there are no studies in mice that examined specifically neurons projecting from the ventral CA1 to the BLA in the context of ELS.

The vulnerability of the brain to ELS may be influenced by genes that modulate the timing of neuronal maturation in specific developing circuits, for example *Syngap1* (Clement et al., 2012), *Ahrgap12* (Ba et al., 2016), *Grin3a* (encoding NR3A) (Henson et al., 2012), and *Met* (Peng et al., 2016; Qiu et al., 2014). Yet, none of these genes have been studied in the context of ELS. *Met*, the gene encoding the MET receptor tyrosine kinase, regulates cortical and hippocampal circuit morphology and synaptic maturation. MET is enriched at developing synapses (Eagleson et al., 2013) in hippocampal, neocortical and other forebrain structures during normal circuit formation in mice and non-human primates (Judson et al., 2009, 2011a). Complete or partial deletion of *Met* in the brain alters neuronal morphology in *Met*-expressing pyramidal neurons in CA1 of the hippocampus and the anterior cingulate cortex (Judson et al., 2010; Qiu et al., 2014), cued fear conditioning and anxiety-like behavior (Thompson and Levitt, 2015), intracortical connectivity (Qiu et al., 2011), and leads to precocious hippocampal excitatory synaptic maturation (Peng et al., 2016; Qiu et al., 2014). Studies in humans are consistent with a conserved function for MET in these circuits. A single nucleotide polymorphism (SNP; rs1858830 '*C*' allele) in the promoter of the *MET* gene reduces *MET*/MET expression in the neocortex and in peripheral monocytes (Campbell et al., 2006, 2007; Heuer et al., 2011; Jackson et al., 2009; Voineagu et al., 2011). Whereas the SNP is associated with increased risk of autism spectrum disorders (ASD) (Campbell et al., 2006), data most pertinent to the present studies are the findings of altered structural (Hedrick et al., 2012) and functional connectivity (Rudie et al., 2012). The latter neuroimaging study revealed a striking interaction of ASD diagnosis and '*C*' allele dosage, suggesting that other (environmental) factors may affect functional and diagnostic outcomes.

Here, we have addressed whether reduced expression of *Met* in the central nervous system interacts with ELS to impact more robustly than either alone, social-emotional behaviors and the morphology of vHC-BLA projection neurons in mice. We show that ELS alone reduced the number of social interactions, and in $Met^{+/-}$ mice, anxiety-like behaviors were decreased and contextual fear memory was impaired. In pyramidal vHC-BLA projection neurons, ELS and $Met^{+/-}$ genotype independently decreased dendritic complexity, whereas ELS in $Met^{+/-}$ mice resulted in a paradoxical increase in complexity compared to non-stressed $Met^{+/-}$ mice. We discuss possible unique mechanisms that relate to CA1 neuronal maturation at the time of ELS, and may underlie the dissociation of behavioral and morphological G × E effects.

2. Materials and methods

2.1. Animals

All animal procedures were approved by the Institutional Animal Care and Use Committee at the University of Southern California, and were carried out in accordance with the National Institutes of Health 'Guide for the Care and Use of Laboratory Animals'. Efforts were made to minimize animal suffering and to reduce the number of mice used for experiments. C57BL/6J mice were housed in 'JAG' mouse cages (Allentown Inc., NJ) in a vivarium on a 12-h light/dark cycle, and temperature and humidity levels maintained at 20–22 °C and 40–60%, respectively. The mice had *ad libitum* access to food and water. Only male mice were analyzed for this study. Litter sizes were standardized across conditions by using second litters of mice. $Met^{fx/fx}$ females were mated with $Nestin^{Cre}$ males, all of which are on a C57Bl/6J background. Litters consist of an approximately similar proportion of $Met^{fx/+}$ (Control) and heterozygous $Nestin^{Cre}/Met^{fx/+}$ ($Met^{+/-}$) pups, the latter expressing approximately 50% of normal MET levels (Thompson and Levitt, 2015). The dams do not express *Cre*, and are no different than wild-type mice behaviorally. Three independent cohorts of mice were used for evaluating MET protein expression, behavioral tests, and morphological analyses. Investigators were blind to genotype and environment experienced by each mouse during tissue collection, behavioral and morphological procedures, and data collection. Weaned mice were genotyped as described in Judson et al. (2009), with a final elongation step of the 320 base pair $Nestin^{Cre}$ PCR product of 7 min, and denaturation steps during the Met^{fx} amplification cycles of 1 min.

2.2. Early life stress paradigm

Details of the paradigm used in the current study are reported in Heun-Johnson and Levitt (2016), based on methods reported in Rice et al. (2008). Briefly, ELS is induced by inserting a wire mesh (#RWF75JMV, Allentown Inc., NJ) into the cage on postnatal day (P)2, and providing the dams with two-thirds (1.8 g) of a nestlet square (Ancare Corp, NY). Control cages lacked the wire mesh insert, and contained standard amount of bedding and one nestlet square. All litters were culled to three males and two females on P2. ELS and Control litters were placed into a fresh control cage environment on P9. Additional cage changes were carried out on P16, and at time of weaning (P21).

2.3. Immunoblot analysis of MET protein expression in hippocampus

Whole hippocampal tissues from P9 mice were homogenized using a glass homogenizer (Wheaton) in ice cold homogenization buffer (10 mM Tris-HCl, pH7.4, 1% SDS, 1% protease inhibitor cocktail (#8340, Sigma)), 1% phosphatase inhibitor 2 (#5726, Sigma). The homogenate was centrifuged for 15 min at 1000 × g at 4 °C, and the supernatant diluted with 5x final sample buffer and centrifuged at 13,000 g. Forty microgram total protein was loaded per lane on a 7.5% acrylamide/bis gel, and transferred to nitrocellulose membrane. After blocking with blotto (5% #9999S Cell Signaling in phosphate-buffered saline), anti-MET antibody (#8057, 1:3000, Santa Cruz Biotechnology), and secondary antibody (#715-035-150, 1:5000, Jackson ImmunoResearch) was used for immunodetection, followed by Femto chemiluminescent substrate (#34095, ThermoFisher). The signal was analyzed using a CCD camera (UVP BioImaging System) and VisionWorksLS software (VisionWorks). The immunostaining process was repeated for anti-α-Tubulin protein (#CP06, 1:200,000, EMD Millipore) to normalize anti-MET signal.

2.4. Behavioral tests

Standard protocols were used for behavioral testing occurring in the

afternoon of the light cycle, as described in Thompson and Levitt (2015) with modifications. Mice were first tested on an elevated-plus maze (EPM) (P58-67) to measure anxiety-like behavior, then in a direct social interaction test (DSI; P68-74), and finally in a contextual fear conditioning test (from P74-80 onward). Mice rested for at least one week between tests. General activity levels were measured at least 24 h prior to surgery in the cohort designated for morphological analyses (P52-55). All behavioral assays were run and scored by an observer who was blind to genotype and rearing status. See Supplementary Methods for more details.

2.5. Intra-amygdalar injection of fluorescent tracer

Details of the methods described here are provided in Supplementary Methods. Briefly, P55-56 mice were deeply anesthetized and placed in a stereotaxic apparatus. Small holes were drilled in the skull above the BLA (−1.34 mm caudal, 3.3 mm lateral from Bregma), and a pulled glass micropipette was lowered 4.4 mm from the dura mater. Using a Narishige IM-200 microinjector and compressed nitrogen, 50–100 nl red fluorescent beads (Lumafluor, Inc.) was expelled, and after slowly raising the micropipette following a 10-min wait, the procedure was repeated in the other hemisphere. On the following day, cage mates were reunited in their home cage. Mice were euthanized on P60, to allow for the tracer to be transported retrogradely to vHC CA1 neurons after tracer injection.

2.6. Preparation of slices for single cell injections

At P60, mice were deeply anesthetized and transcardially perfused with approximately 5 ml of cold 1% paraformaldehyde (PFA), followed by 60 ml cold 4% PFA + 0.125% gluteraldehyde (Dumitriu et al., 2011). After perfusion, the brain was removed from the skull, and divided into three equal segments. The brain segments were post-fixed in 4% PFA/0.125% gluteraldehyde for 4 h on ice. After post-fixation, the posterior segment containing the vHC was sectioned horizontally on a vibratome (#VT1200S, Leica) in ice cold PBS at a thickness of 250 μm. Sections were kept in 0.1% NaN_3 in PBS at 4 °C until cell injections.

2.7. Evaluation of amgydalar injection site

Specific brains to be used for cell injections were determined by evaluating the tracer injection site in the BLA. Details are provided in Supplementary Methods. Briefly, after post-fixation, brain segments containing the BLA were cryoprotected, frozen in dry ice-cooled isopentane, and stored at −80 °C. Coronal cryostat sections of 20 μm were mounted, and imaged with a Zeiss Axioplan 2 microscope. The shape and edges of the amygdala (determined by a change in cell density with DAPI staining) were used as the primary determinants of the anterior-posterior level and compared with images from the Paxinos Mouse Brain Atlas (Franklin and Paxinos, 2007). Only brains with fluorescent dye present in the BLA and not in adjacent structures were used for subsequent cell fill injections (Control $n = 5$; ELS $n = 7$; $Met^{+/-}$ $n = 6$; $Met^{+/-}$ × ELS $n = 6$, from 16 independent litters). All groups (Control, ELS, $Met^{+/-}$, $Met^{+/-}$ × ELS) were represented equally among the anterior-posterior axis of the BLA (Supplementary Fig. 1).

2.8. Intracellular injections

Details of the methods described here are provided in Supplementary Methods. Briefly, tracer-positive, vHC CA1 pyramidal neurons were injected with Lucifer Yellow dye, on a Leica DM LFSA microscope, using a borosilicate micropipette with filament and an Ag-wire micropipette holder connected to a Kation Scientific M1200 microiontophoresis unit (modified range of 0–50 nA). The micropipette was diagonally advanced into the tissue slices using a Sutter #MP-225 micromanipulator. Cells were injected with 0.1–5 nA of continuous negative current for approximately 5 min, until the neuron was fully filled.

2.9. Whole cell imaging, reconstruction and analysis

Brain slices with dye-injected cells were mounted between a glass microscope slide and a #1.5 glass coverslip (#48393194, VWR) in Prolong Gold Antifade Mountant (ThermoFisher #P36930), with two spacers of 120 μm thickness each (EMS Diasum #70327-13S) to prevent compression of the sections. The slices were cured at least 24 h before imaging. Neurons were visualized using a Zeiss Axioscope equipped with automatic X-Y stage and Z-meter driven by a Neurolucida system (MicroBrightField), and an epifluorescent light source with FITC and CY3 filters under a 20× objective. Morphology of Lucifer Yellow filled neurons was captured with a high sensitivity monochrome camera (Retiga, 2000R, Qimaging). The reconstructed neurons were analyzed using NeuroExplorer (NeuroLucida) to obtain total dendritic length of apical and basal arbors, as well as dendritic complexity by performing a Sholl analysis with three-dimensional spheres spaced 10 μm apart starting at the cell body (Sholl, 1953). Neurons were included in whole cell analyses if they were at sufficient depth from the surface to include the complete dendritic arbor; i.e. if the cell soma was approximately in the center of the difference between the deepest dendrites and the most superficial dendrites, and dendrites were not cut off at the slice surface. The number of neurons included for each animal are listed in Supplementary Table 1.

2.10. Spine imaging, reconstruction and analysis

Details of the methods described here are provided in Supplementary Methods. Briefly, Lucifer Yellow dye was amplified with anti-Lucifer Yellow antibody, Biotin-conjugated secondary antibody, and Alexa Fluor 488-conjugated streptavidin. The slices were mounted with two 120 μm spacers to prevent compression. Images with a voxel size of 101 nm (x) × 101 nm (y) × 160 nm (z-step size) of spines were obtained with a Zeiss confocal microscope (LSM 710) with 63 × 1.40 NA oil-immersion objective. Images were processed with attenuation correction and 3D deconvolution and analyzed with NeuronStudio software (Rodriguez et al., 2006; Wearne et al., 2005). Spines, and their length, volume and type (mushroom, stubby or thin) were automatically detected and analyzed using NeuronStudio, and subsequently adjusted manually for correct spine placement and detection. Subsequently manually-added spines were excluded from spine type and volumetric spine analysis (with Rayburst) due to an inherent difference in contrast detection in NeuronStudio. The manually-added spines, however, were included in spine length and spine density analyses. The total length of dendrite segments analyzed for each animal, and the total spine count are listed in Supplementary Table 1. All analyses of neuron and spine morphology were completed by an observer blind to genotype and rearing status.

2.11. Statistical analyses

Data were analyzed using SPSS/PASW 22 (IBM) and GraphPad Prism 6. MET protein expression, distance traveled in activity chamber, DSI social interaction duration, DSI number of social interactions, EPM time in arm, EPM arm entry, fear conditioning freezing, dendritic length, spine volume, spine density, spine length, and spine type, were analyzed using a two-way ANOVA (genotype × environment). Furthermore, to explore indications of potential interactions that are of clinical relevance, but that we did not have the statistical power to detect, we calculated the Cohen's *d* effect size by dividing the difference between two relevant group means by their pooled standard deviation. A three-way repeated measures ANOVA was used to analyze dendritic complexity for Sholl analysis (genotype × environment × distance from soma), and spine type density and proportion of total

Table 1
Met$^{+/-}$ mice that experienced ELS show an increased number of affected behavioral domains. Summary of behavior test results in experimental groups compared to Control group. The outcomes and direction of the difference (↑ = increased, ↓ = decreased, ↔ = unchanged) are indicated for anxiety-like behavior, social behavior and fear conditioning measurements.

		Met$^{+/-}$	ELS	*Met*$^{+/-}$ × ELS
Anxiety-like behavior	Open-arm duration EPM	↑[a]	↔	↑[a]
	Open-arm entries EPM	↑[a]	↔	↑[a]
	Unprotected head dips EPM	↑[a]	↔	↑[a]
	Protected head dips EPM	↔	↔	↔
Social behavior	Number of social interactions	↔	↓[b]	↓[b]
	Duration of social interactions	↔	↔	↔
Fear conditioning	Contextual fear acquisition	↔	↔	↔
	Contextual fear memory	↓[a]	↔	↓[a]
	Contextual fear extinction	↔	↔	↔

[a] Main effect of genotype.
[b] Main effect of ELS.

(genotype × environment × spine head volume bin/spine type). Tukey and Sidak multiple comparisons tests were performed after ANOVA tests (alpha = 0.05) when appropriate. Data are presented as mean ± standard error of the mean (SEM). A Pearson correlation analysis was performed to analyze the correlation between EPM open-arm time and the number of unprotected head dips, and regression analysis to determine whether the regression coefficients (slope) are different.

3. Results

3.1. Four different groups of mice were evaluated

1) Control: wild-type mice raised in standard rearing conditions;
2) ELS: wild-type mice raised in a limited bedding, early-life stress environment;
3) *Met*$^{+/-}$: mice with reduced *Met* expression raised in standard rearing conditions;
4) *Met*$^{+/-}$ × ELS: mice with reduced *Met* expression raised in a limited bedding, early-life stress environment. The results of all behavior tests are summarized in Table 1.

3.2. MET protein levels

MET protein levels normally decrease to very low levels during the third postnatal week (Eagleson et al., 2016; Judson et al., 2009), and thus, MET protein expression was analyzed immediately after conclusion of the ELS period at P9 to determine possible direct effects of ELS. Immunoblot densitometry analysis showed a main effect of *Met*$^{+/-}$ genotype, but not ELS, on the levels of MET protein in P9 hippocampus (*Met*$^{+/-}$: $F_{1,34} = 194.1$, $p < 0.001$; ELS: $F_{1,34} = 1.08$, $p = 0.307$) (Fig. 1). There was no interaction between these two factors ($F_{1,34} = 0.39$, $p = 0.539$). These results indicate that ELS does not exert its effects on behavior or neuronal morphology directly through alterations in MET protein expression in wild-type or *Met*$^{+/-}$ mice during development.

3.3. Anxiety-like behavior

Mice were tested for changes in anxiety-like behavior using three different measures on the EPM: time spent in the open arm, number of open-arm entries, and head dips. Two-way ANOVA showed a main effect of *Met*$^{+/-}$ genotype on the time spent in the open arm ($F_{1,62} = 5.46$, $p < 0.05$; Fig. 2A), but no main effect of ELS ($F_{1,62} = 1.44$, $p = 0.234$) or interaction effect ($F_{1,62} = 0.60$, $p = 0.443$). A main effect of *Met*$^{+/-}$ genotype was also present for the number of open-arm entries ($F_{1,62} = 7.17$, $p < 0.01$; Fig. 2B), and the number of unprotected head-dips ($F_{1,62} = 6.97$, $p < 0.05$; Fig. 2C). A within-ELS group comparison showed a medium and large effect size (Cohen's $d = 0.7$ and 0.8) of *Met*$^{+/-}$ genotype for open-arm time and number of unprotected head dips, resulting in 9% more time spent in the open arm and five more unprotected head-dips, respectively. Logically, a significant linear positive correlation existed between open-arm time and the number of unprotected head dips (wild-type: $r = 0.98$, *Met*$^{+/-}$: $r = 0.90$, both $p < 0.001$). However, the slopes between the two groups are different (wild-type = 0.42; *Met*$^{+/-}$ = 0.62, $p < 0.001$), suggesting that an increase in open-arm time was accompanied by a larger increase of unprotected head dips in *Met*$^{+/-}$ mice than in wild-type mice (Fig. 2D). The number of protected head dips did not change (Supplementary Fig. 2). No effect of *Met*$^{+/-}$ genotype or ELS was observed on the number of closed-arm entries (*Met*$^{+/-}$ genotype: $F_{1,62} = 2.78$, $p = 0.101$; ELS: $F_{1,62} = 2.090$, $p = 0.153$; interaction: $F_{1,62} = 0.05$, $p = 0.824$; Fig. 2B), suggesting ELS or *Met*$^{+/-}$ genotype did not affect general activity levels. This was confirmed by a lack of change in total distance traveled in the activity chamber (Supplementary Fig. 3).

3.4. Direct social interaction

A 6-min direct social interaction test between experimental mice and same-sex juvenile 129S1/SvImJ mice was performed to measure changes in sociability. Whereas the total duration of social interactions was unaffected (Supplementary Fig. 4), we observed a main effect of ELS on the *number* of social interactions initiated by the experimental adult ($F_{1,62} = 11.59$, $p < 0.01$; Fig. 2E). There was no main effect of *Met*$^{+/-}$ genotype or interaction between the two factors (*Met*$^{+/-}$ genotype: $F_{1,62} = 0.15$, $p = 0.700$, interaction: $F_{1,62} = 0.86$, $p = 0.357$). Within-genotype comparisons revealed a large effect size of ELS with a reduction of eight interactions in *Met*$^{+/-}$ mice (Cohen's $d = -1.2$), and six interactions in wild-type mice (Cohen's $d = -0.9$).

3.5. Contextual fear memory

Contextual fear conditioning was performed to determine whether *Met*$^{+/-}$ genotype and ELS affect fear acquisition, memory and extinction. We observed a main effect of *Met*$^{+/-}$ genotype on fear memory

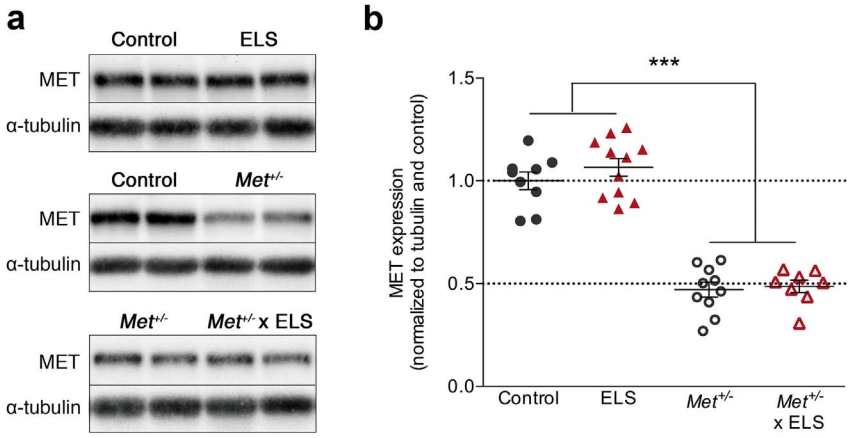

Fig. 1. MET protein expression was decreased in hippocampus of P9 $Met^{+/-}$ mice, and did not change due to ELS. (a) Representative immunoblots with anti-MET and anti-α-tubulin antibody labeling of hippocampal tissue from P9 Control and $Met^{+/-}$ mice (top), Control and ELS mice (middle), and $Met^{+/-}$ and $Met^{+/-}$ × ELS mice (bottom). (b) Compared to Control mice, normalized MET protein expression in P9 hippocampus was decreased with approximately 50% in $Met^{+/-}$ mice and $Met^{+/-}$ × ELS mice ($p < 0.001$). Within genotype, ELS did not alter MET protein expression. Number of animals per group: Control $n = 9$; ELS $n = 11$; $Met^{+/-}$ $n = 10$; $Met^{+/-}$ × ELS $n = 8$. Data are presented as mean ± SEM. ***$p < 0.001$.

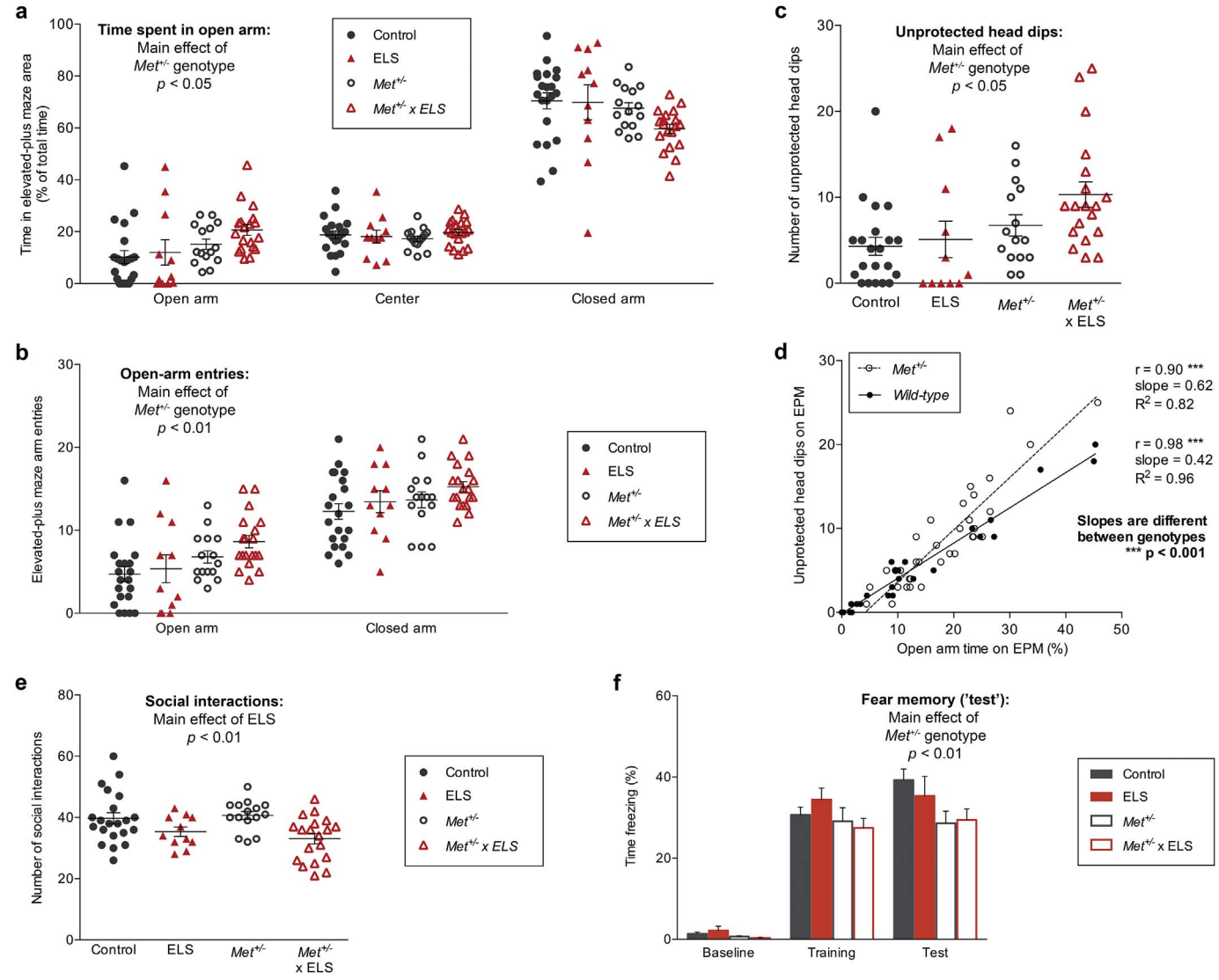

Fig. 2. Behavioral tests revealed an increased number of affected behavioral domains in adult $Met^{+/-}$ × ELS mice. (a) A main effect of $Met^{+/-}$ genotype was observed on time spent in the open arm ($p < 0.05$) and (b) open-arm entries ($p < 0.01$) on the elevated plus maze, whereas the number of closed-arm entries was not affected. (c) $Met^{+/-}$ genotype also increased the number of unprotected head dips (body in open arm of the elevated-plus maze) ($p < 0.05$). (d) The increase in the number of unprotected head-dips by $Met^{+/-}$ mice is only partially explained by time spent in the open arm, as a higher number of unprotected head dips is predicted based on open-arm time in these mice compared to wild-type mice ($p < 0.001$). Non-ELS and ELS data were combined for each respective genotype for this analysis. (e) A main effect of ELS was observed on the number of social interactions ($p < 0.01$) in a 6-min direct social interaction test. (f) A main effect of $Met^{+/-}$ genotype was observed on fear memory (a reduction in the amount of freezing 24 h after fear acquisition) in a contextual fear conditioning paradigm ($p < 0.01$). Number of animals per group: Control $n = 21$; ELS $n = 11$; $Met^{+/-}$ $n = 15$; $Met^{+/-}$ × ELS $n = 19$. Data are presented as mean ± SEM. **$p < 0.01$, ***$p < 0.001$.

('test') ($F_{1,62}$ = 6.53, p < 0.05; Fig. 2F), but no main effect of ELS ($F_{1,62}$ = 0.23, p = 0.64), nor an interaction between the two factors ($F_{1,62}$ = 0.53, p = 0.47). Within ELS-group comparisons did not reveal statistical differences between genotypes. There was a medium effect size of $Met^{+/-}$ genotype (Cohen's d = 0.7), resulting in 9% less time freezing by $Met^{+/-}$ mice compared to Control mice. No main or interaction effects of $Met^{+/-}$ genotype or ELS were observed on fear acquisition ('training') (Fig. 2F) or the extinction of fear memory

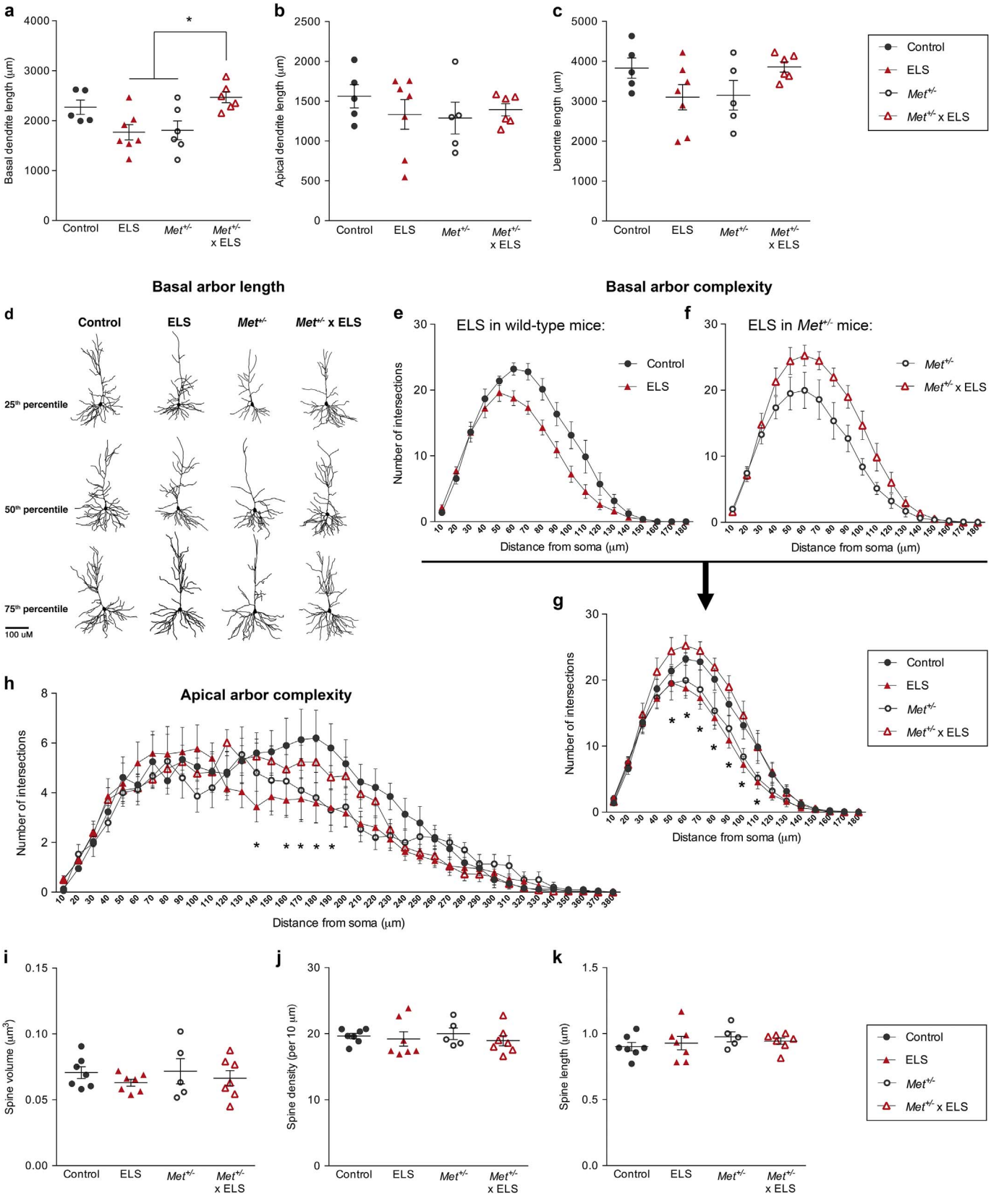

(caption on next page)

Fig. 3. *Met*$^{+/-}$ genotype and ELS interact to alter dendritic morphology of vHC CA1 pyramidal neurons that project to the BLA, at P60. (a) Dendritic length of the basal arbor is increased due to ELS in *Met*$^{+/-}$ mice compared to non-stressed *Met*$^{+/-}$ mice or wild-type mice that had experienced ELS, whereas (b) dendritic length of the apical arbor and (c) the complete neuronal arbor is unaffected. (d) Representative examples with basal arbor lengths close to the 25th, 50th and 75th percentile in their respective experimental groups are provided to show the distribution of changes in basal dendritic length. (e) As a result of ELS, basal arbor complexity is reduced in wild-type mice and (f) increased in *Met*$^{+/-}$ mice, shown by a decrease in the number of intersections in Sholl analysis. In contrast, ELS in *Met*$^{+/-}$ mice leads to an increased complexity compared to non-stressed *Met*$^{+/-}$ mice. (g) Graphs (e) and (f) are combined to compare all four groups. See Results section 3.5 for specific significant differences between groups at each distance from the soma. (h) Similar to the basal arbor, apical arbors were impacted by *Met*$^{+/-}$ genotype, ELS or a combination of both factors. See Results section 3.5 for specific significant differences between groups at each distance from the soma. Number of animals per group: Control $n = 5$; ELS $n = 7$; *Met*$^{+/-}$ $n = 6$; *Met*$^{+/-}$ × ELS $n = 6$. Each individual data point is the average of 2.3 neurons per animal (range 1–4). (i–k) ELS, *Met*$^{+/-}$ genotype or a combination of these factors did not affect (i) spine head volume, (j) spine density, or (k) spine length of spines on basal arbors of vHC CA1 pyramidal neurons that project to the BLA. Number of animals per group: Control $n = 7$; ELS $n = 7$; *Met*$^{+/-}$ $n = 5$; *Met*$^{+/-}$ × ELS $n = 7$. Each individual data point is an average of two neurons per animal. Data are presented as mean ± SEM. *$p < 0.05$.

(Supplementary Fig. 5).

3.6. Dendritic morphology of BLA-projecting ventral CA1 neurons

Retrogradely labeled ventral CA1 neurons projecting to the BLA, were analyzed for potential changes in basal and apical dendritic architecture. Dye-filled apical arbors of tracer-positive neurons were mainly positioned in the stratum radiatum and lacked a distinct apical tuft as expected based on their projection target to the BLA (Graves et al., 2012). We observed an interaction effect of *Met*$^{+/-}$ genotype and ELS on dendritic length of basal arbors ($F_{1,20} = 14.27$, $p < 0.01$, Fig. 3A). Post-hoc tests revealed that the dendritic length of basal arbors in *Met*$^{+/-}$ × ELS mice was greater compared to the individual *Met*$^{+/-}$ and ELS groups ($p < 0.05$). Neither apical dendritic length (Fig. 3B), nor total dendritic length (Fig. 3C) was significantly changed as a result of ELS or *Met*$^{+/-}$ genotype. Examples of representative neuron tracings with basal lengths close to the 25th, 50th, and 75th percentile are presented in Fig. 3D.

Factorial repeated measures ANOVA of Sholl analyses showed that for the basal arbor, an interaction effect exists between *Met*$^{+/-}$ genotype and ELS on dendritic arbor complexity. This interaction effect is not uniform across the basal dendritic tree, analyzed by examining the interaction between *Met*$^{+/-}$ genotype, ELS environment and distance from the soma ($F_{2.5,49.8} = 5.41$, $p < 0.01$; Mauchly's test indicated that the assumption of sphericity had been violated, thus a Greenhouse-Geisser correction was applied to *df*; Fig. 3E–G). Subsequent analyses revealed that ELS alone reduced basal arbors complexity at 70–110 μm from the cell body ($p < 0.05$). Compared to either ELS or *Met*$^{+/-}$ mice, *greater* basal arbor complexity was observed at 50–110 μm from the cell body in the *Met*$^{+/-}$ × ELS interaction group ($p < 0.05$). Basal arbor complexity in the *Met*$^{+/-}$ × ELS interaction group was not significantly different from Control mice.

Sholl analysis revealed a similar interaction effect regarding apical arbor complexity (after Greenhouse-Geisser correction, $F_{4.7,89.3} = 2.43$, $p < 0.05$; Fig. 3H). In ELS mice, apical arbor complexity was reduced at 140 μm and 160–190 μm from the cell body ($p < 0.05$) compared to Control mice. Similar to ELS in wild-type mice, *Met*$^{+/-}$ genotype alone resulted in reduced complexity of the apical arbor, but at 180–190 μm from the cell body ($p < 0.05$) compared to Control mice. Consistent with what was observed for basal arbors, apical arbor complexity was not significantly different in *Met*$^{+/-}$ × ELS mice compared to Control mice. Results of the Sholl analyses suggest that ELS induces dendritic architecture changes in *Met*$^{+/-}$ mice that are distinct from those in wild-type mice.

3.7. Spine characteristics are unaffected by *Met*$^{+/-}$ or ELS

High resolution reconstruction of dendritic spines on filled ventral CA1 neurons was performed for all experimental groups, followed by quantitative morphometry. There were no main or interactive effects of ELS and *Met*$^{+/-}$ on spine volume (Fig. 3I), spine density (Fig. 3J) and spine length (Fig. 3K) measurements. In addition, no significant interaction effects between ELS, *Met*$^{+/-}$ genotype, and spine type proportion ($F_{4.7,\ 34.2} = 0.86$, $p = 0.51$, after Greenhouse-Geisser correction) or frequency distribution of spine head volume ($F_{4.7,\ 32.7} = 0.88$, $p = 0.50$, after Greenhouse-Geisser correction) was present, although a trend for a main effect of ELS was observed on the proportion of thin spines ($p = 0.06$) (Supplementary Figs. 6 and 7, respectively).

4. Discussion

The present study was designed to determine whether reduced expression of a gene that is involved in synaptic maturation in the hippocampus could serve as an additional risk factor for enduring behavioral and neuronal morphology changes when combined with ELS. Using a well-characterized mouse model, this G × E study reveals that different measures of behavior and ventral CA1 neuronal architecture respond uniquely to a combined developmental perturbation of reduced *Met* expression and ELS. We found that ELS impaired social interactions equivalently in control and *Met*$^{+/-}$ mice, and reduced *Met* expression decreased anxiety-like behavior and contextual fear learning regardless of rearing environment. Furthermore, neuronal morphology was impacted by an interaction effect of reduced *Met* expression and ELS;

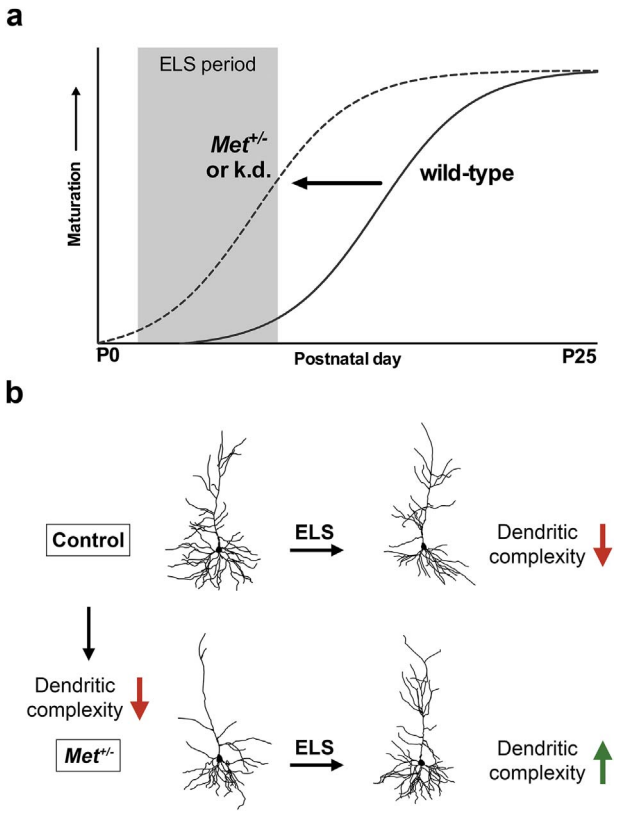

Fig. 4. (a) Precocious neuronal maturation due to reduced expression of *Met* results in a *de facto* shift in timing during which ELS occurs in *Met*$^{+/-}$ mice compared to wild-type mice. k.d. = knock down. (b) Possibly due to this altered maturational state of neurons, ELS results in decreased dendritic complexity of vHC CA1 neurons that project to the BLA in wild-type mice, whereas ELS causes an increase in dendritic complexity and length in *Met*$^{+/-}$ mice.

either ELS or *Met*$^{+/-}$ genotype decreased dendritic complexity, whereas ELS in *Met*$^{+/-}$ mice resulted in a paradoxical increase in complexity compared to non-stressed *Met*$^{+/-}$ mice.

We hypothesize that a reduction in *Met* expression alters the sensitivity of developing CA1 hippocampal neurons to ELS. Because of the role of MET in the timing of synaptic maturation of hippocampal neurons (Peng et al., 2016; Qiu et al., 2014), it is possible that a precocious shift towards earlier maturity of MET-expressing brain circuits influences the response to early postnatal ELS (Fig. 4A). Importantly, there were unexpected differences in G × E interaction effects on behavior and vHC CA1 neuronal architecture, suggesting a more complex regulation of how ELS and genetic risk interact at the level of individual phenotypes.

4.1. Phenotypic effects of reduced Met expression

Reduced expression of *Met* has been implicated in modulating the maturational state of hippocampal neurons (Peng et al., 2016; Qiu et al., 2014), synaptic input of intralaminal cortical connectivity (Qiu et al., 2011), neuronal morphology (Judson et al., 2010; Qiu et al., 2014), synaptogenesis (Eagleson et al., 2016), and specific behaviors (Okaty et al., 2015; Thompson and Levitt, 2015). Here, main effects of *Met*$^{+/-}$ genotype on fear memory and anxiety-like behavior replicate, in part, previous studies in which *Met*$^{+/-}$ mice exhibited reduced anxiety-like behavior, and impaired fear acquisition and memory (Thompson and Levitt, 2015). The lack of effect on contextual fear acquisition in the current study, but with replication of the disruption of fear memory will require further investigation to understand possible technical or other origins of the differences. In the current study, we demonstrated that the *Met*$^{+/-}$ genotype produces an increase in exploration of unprotected areas of the elevated-plus maze, as reported previously (Thompson and Levitt, 2015). In the latter study, there was a significant difference in center time, with a trend in the number of open arm entries; increased time spent in open arms was revealed in the present study. Again, this may be due to differences in the individuals who ran the behavioral tasks, or even the differences in vivaria in which the tasks were performed. Lastly, the lack of a main effect of *Met*$^{+/-}$ genotype on social interaction is consistent with previous results using a 3-chamber task (Thompson and Levitt, 2015).

Reducing or eliminating MET receptor signaling alters dendritic growth in subsets of neocortical pyramidal and hippocampal CA1 neurons (Gutierrez et al., 2004; Judson et al., 2010; Lim and Walikonis, 2008; Peng et al., 2016; Qiu et al., 2014), similar to the findings reported here for vHC-BLA neurons. Further, *Met* deletion in the dorsal pallium leads to an increase in spine head volume on basal dendrites in the anterior cingulate cortex, without changes in spine density or spine length (Judson et al., 2010). Similarly, partial reduction of *Met* expression in the dorsal CA1 region of the hippocampus leads to an increase in volume of spine heads on the apical arbor in four-week old mice, although in this region there is an accompanying decrease in spine density (Qiu et al., 2014). This may reflect distinct regulatory roles for MET signaling in dorsal hippocampal versus neocortical pyramidal neurons. Here, we did not observe a change in any spine measure in a subpopulation of retrogradely-labeled ventral CA1 neurons that project to BLA, indicating even further layers of complexity in the impact of MET on neuronal morphology, with distinct outcomes in closely related neuron populations. Technical limitations of BLA-injected tracer not labeling all ventral CA1 projection neurons precluded a comparison of labeled and unlabeled neuron neighbors in the present study.

4.2. Phenotypic effects of ELS

ELS effects on adult rodent social-emotional behavior have been studied widely. First, analogous to our results, typically there is a decrease in social interaction observed after ELS (Bouet et al., 2011; Raineki et al., 2012, 2015; Santarelli et al., 2014; Tsuda and Ogawa, 2012; Tsuda et al., 2014; van der Kooij et al., 2015; Venerosi et al., 2003), although several reports show no change in the duration of social interaction (Franklin et al., 2011; Harrison et al., 2014; Tsuda et al., 2011; Zoicas and Neumann, 2016). Second, ELS appears to have limited effectiveness in altering anxiety-like behavior, as many groups report no change in duration spent in the open arm of an EPM (Liu et al., 2016; van der Kooij et al., 2015; van Heerden et al., 2010; Venerosi et al., 2003; Wang et al., 2012; Zoicas and Neumann, 2016) and the open section of the elevated-zero maze (Harrison et al., 2014). These findings are consistent with ours that ELS alone did not alter anxiety-like measures in wild-type mice. Third, a few groups have described effects of maternal separation and limited bedding on fear conditioning in adult mice. Specifically, Wang et al (2011a,b) and Kanatsou et al. (2016) reported that ELS reduced freezing, 24 h after combining a tone and foot shock in the same context. However, ELS did not affect acquisition, nor extinction of a fear memory in two recent studies using contextual (Kanatsou et al., 2016) and cued (Arp et al., 2016; Zoicas and Neumann, 2016) fear conditioning paradigms. The lack of ELS-induced impairment of fear memory in the current study was somewhat unexpected, but may be due to differences in methodology that tap into overlapping, but non-identical circuits (Smith and Bulkin, 2014), as we induced a contextual fear association in the absence of a tone.

In wild-type animals, ELS consistently reduces dendritic complexity of apical pyramidal neurons in the mouse neocortex and dorsal and intermediate hippocampus (Brunson et al., 2005; Ivy et al., 2010; Liao et al., 2014; Liu et al., 2016; Yang et al., 2015), similar to the findings reported in the current study for vHC-amygdalar neurons. Complexity of basal arbors is also often reduced (Brunson et al., 2005; Chocyk et al., 2013; Liao et al., 2014), or unaffected (Ivy et al., 2010; Liu et al., 2016; Yang et al., 2015). In addition, apical dendritic length is generally reduced, but basal length unaffected, as a result of ELS (Bock et al., 2005; Brunson et al., 2005; Ivy et al., 2010; Liao et al., 2014; Liu et al., 2016; Yang et al., 2015), the latter of which is consistent with our findings. However, the lack of reduction in apical arbor length in the present study is unexpected, but may be due to the specific nature and morphology of these neurons, as these amygdala-projecting neurons receive different input on apical branches than other neuronal populations in the CA1 (Graves et al., 2012). The developmental timing of ELS appears to be a critical variable in defining neuronal responses; early postnatal stressors in previous studies have resulted in reduced dendritic length (Bock et al., 2005; Chocyk et al., 2013; Eiland and McEwen, 2012; Romano-Lopez et al., 2015), whereas exposure to stressors later postnatally induced a paradoxical increase in dendritic length (Bock et al., 2005; Xie et al., 2013). Similarly, ELS generally induces a decrease or no change in spine density in CA3 or CA1 hippocampus, respectively (Liao et al., 2014; Monroy et al., 2010; Wang et al., 2011b, 2013), but later ELS increases spine density (Bock et al., 2005; Xie et al., 2013). Thus, perhaps the increased growth of dendrites in *Met*$^{+/-}$ mice exposed to ELS was predictable, given that hippocampal CA1 neurons with reduced *Met* expression exhibit a more mature phenotype (Peng et al., 2016; Qiu et al., 2014).

4.3. Genetic factors that influence responses to ELS

As noted above, the timing of ELS exposure appears to affect the sensitivity to early adverse experiences. Studies by Bock et al. (2005) and Xie et al. (2013) provide support for the hypothesis that ELS in older pups leads to somewhat unexpected, opposite effects on dendritic morphology. One hypothesis that aligns with these findings is that the maturational state of the brain is a factor in determining response to ELS. This provides insight into the possible mechanisms through which reduced expression of *Met* interact with ELS to affect outcome. For example, there is substantial biochemical and electrophysiological evidence that excitatory synaptic function of hippocampal neurons in *Met*$^{+/-}$ mice matures precociously (Peng et al., 2016; Qiu et al., 2014),

a hypothesis first proposed by Judson et al. (2011b). Specifically, CA1 neurons that had reduced or no expression of *Met* exhibited more mature electrophysiological properties, such as a greater AMPA:NMDA current ratio, an increased amplitude of miniature excitatory post-synaptic currents, a lower proportion of silent synapses, and precocious expression levels of membrane-associated AMPA and NMDA receptor subunits. Early maturation phenotypes were evident during the first and second postnatal week, but normalized to wild-type levels by P26-28. Here, given the results of the present study, we hypothesize that the effects of ELS during the first week in $Met^{+/-}$ mice more closely mimic the effects of ELS in the second week in wild-type mice, when synaptic connectivity is more mature. Consistent with this and the studies by Bock et al. (2005) and Xie et al. (2013), analyses in $Met^{+/-}$ mice exposed to ELS revealed an increase in dendritic complexity (Fig. 4B). This finding provides additional evidence that MET signaling regulates important aspects of the functional development of connectivity in circuitry in which the protein is expressed. However, further studies applying ELS during different postnatal time periods will need to be performed to test this hypothesis.

The maturational differences may underlie the morphological responses to ELS in wild-type compared to $Met^{+/-}$ mice, but do not explain the behavioral findings. Results from one study show that social behavior is equally impaired by early (P2-9) or late (P10-17) ELS (van der Kooij et al., 2015). Together with the present results, there may not be a generalized response to timing differences in ELS exposure, but rather differential phenotypic sensitivity. The morphological changes in vHC-BLA projection neurons reflect what may be a larger impact on neurons in multiple complex circuits impacted by ELS or a reduction of MET protein. The specific neurons that are the focus of this study are only one of many components that adapt to altered input, such as increased glutamatergic signaling due to ELS (Toya et al., 2014). The adaptation to ELS by a complex neuronal network as a whole will determine specific behavioral changes. Thus, we suggest that it may be too simplistic to associate altered morphological characteristics of one specific projection neuron type to observed changes in behavior. A more comprehensive assessment of other brain regions, e.g. the medial amygdala with its ability to affect social interactions (Lau et al., 2017), is needed to fully understand the relationship of the observed morphological changes to a specific behavior. Nevertheless, the present analysis provides an initial foundation for more experimental studies to understanding interactions at the behavioral and neuroanatomic levels. This will inform future circuit analyses.

Furthermore, ELS impaired social behavior, but $Met^{+/-}$ genotype resulted in impaired contextual fear memory and reduced anxiety-like behavior. These findings in our animal model support a complex picture, in which not all behaviors respond identically. Thus, the underlying circuitry that mediates certain behaviors may be more or less sensitive to combined disruptions of rearing environment and *Met* expression. Human studies would provide insight into how these changes result in enduring effects on behavior. The present findings have translational implications, because MET expression in humans varies by promoter genotype and not clinical diagnosis (Campbell et al., 2006, 2007; Heuer et al., 2011). Thus, for individuals with a *C/C*, or reduced expression genotype, a variety of environmental stressors could result in greater risk for disrupted neurodevelopmental outcomes. Such factors may contribute to the recent G × E findings for ASD risk combining prenatal exposure to air pollutants and *MET* promoter genotype (Volk et al., 2014).

In conclusion, the results of the present G × E study provide new evidence that the MET receptor tyrosine kinase, which mediates aspects of synapse and circuit formation in the forebrain, is a heritable biological factor that can influence neuronal responses to early adversity. Given differences in expression of *MET* in humans based on promoter genotype (*'GG', 'GC' or 'CC'*), incorporating *MET* genotype analysis for clinical studies that examine the effect of ELS on the etiology of mental health and neurodevelopmental disorders may reveal a potential moderator of phenotype effect size that influences heterogeneity across study populations.

Funding and disclosure

The studies were supported by the National Institute of Mental Health under Ruth L. Kirschstein National Research Service Award F31 MH100779 (HH-J), and R01 MH067842 (PL), the Simm/Mann Family Foundation Chair in Developmental Neurogenetics and Simms/Mann Family research fund, WM Keck Chair in Neurogenetics (PL), and the JPB Research Network on Toxic Stress: A Project of the Center on the Developing Child at Harvard University (PL). The authors declare no conflicts of interest.

Acknowledgements

We would like to thank Dr. Shenfeng Qiu, Mariel Piechowicz, Kevin Jiang, and Hojean Yoon for technical assistance, and Drs. Allison Knoll and Kathie Eagleson for critical reading of the manuscript.

Appendix A. Supplementary data

Supplementary data related to this article can be found at http://dx.doi.org/10.1016/j.ynstr.2017.11.003.

References

Almli, L.M., Fani, N., Smith, A.K., Ressler, K.J., 2014. Genetic approaches to understanding post-traumatic stress disorder. Int. J. Neuropsychopharmacol. 17 (2), 355–370. http://dx.doi.org/10.1017/S1461145713001090.

Arp, J.M., Ter Horst, J.P., Loi, M., den Blaauwen, J., Bangert, E., Fernandez, G., Joels, M., Oitzl, M.S., Krugers, H.J., 2016. Blocking glucocorticoid receptors at adolescent age prevents enhanced freezing between repeated cue-exposures after conditioned fear in adult mice raised under chronic early life stress. Neurobiol. Learn Mem. 133, 30–38. http://dx.doi.org/10.1016/j.nlm.2016.05.009.

Ba, W., Selten, M.M., van der Raadt, J., van Veen, H., Li, L.L., Benevento, M., Oudakker, A.R., Lasabuda, R.S.E., Letteboer, S.J., Roepman, R., van Wezel, R.J.A., Courtney, M.J., van Bokhoven, H., Nadif Kasri, N., 2016. ARHGAP12 functions as a developmental brake on excitatory synapse function. Cell Rep. 14 (6), 1355–1368. http://dx.doi.org/10.1016/j.celrep.2016.01.037.

Baram, T.Z., Davis, E.P., Obenaus, A., Sandman, C.A., Small, S.L., Solodkin, A., Stern, H., 2012. Fragmentation and unpredictability of early-life experience in mental disorders. Am. J. Psychiatry 169 (9), 907–915. http://dx.doi.org/10.1176/appi.ajp.2012.11091347.

Bock, J., Gruss, M., Becker, S., Braun, K., 2005. Experience-induced changes of dendritic spine densities in the prefrontal and sensory cortex: correlation with developmental time windows. Cereb. Cortex 15 (6), 802–808. http://dx.doi.org/10.1093/cercor/bhh181.

Bouet, V., Lecrux, B., Tran, G., Freret, T., 2011. Effect of pre- versus post-weaning environmental disturbances on social behaviour in mice. Neurosci. Lett. 488 (2), 221–224. http://dx.doi.org/10.1016/j.neulet.2010.11.033.

Bradley, R.G., Binder, E.B., Epstein, M.P., Tang, Y., Nair, H.P., Liu, W., Gillespie, C.F., Berg, T., Evces, M., Newport, D.J., Stowe, Z.N., Heim, C.M., Nemeroff, C.B., Schwartz, A., Cubells, J.F., Ressler, K.J., 2008. Influence of child abuse on adult depression: moderation by the corticotropin-releasing hormone receptor gene. Arch. Gen. Psychiatry 65 (2), 190–200. http://dx.doi.org/10.1001/archgenpsychiatry.2007.26.

Brunson, K.L., Kramar, E., Lin, B., Chen, Y., Colgin, L.L., Yanagihara, T.K., Lynch, G., Baram, T.Z., 2005. Mechanisms of late-onset cognitive decline after early-life stress. J. Neurosci. 25 (41), 9328–9338. http://dx.doi.org/10.1523/JNEUROSCI.2281-05.2005.

Campbell, D.B., D'Oronzio, R., Garbett, K., Ebert, P.J., Mirnics, K., Levitt, P., Persico, A.M., 2007. Disruption of cerebral cortex MET signaling in autism spectrum disorder. Ann. Neurol. 62 (3), 243–250. http://dx.doi.org/10.1002/ana.21180.

Campbell, D.B., Sutcliffe, J.S., Ebert, P.J., Militerni, R., Bravaccio, C., Trillo, S., Elia, M., Schneider, C., Melmed, R., Sacco, R., Persico, A.M., Levitt, P., 2006. A genetic variant that disrupts MET transcription is associated with autism. Proc. Natl. Acad. Sci. U. S. A. 103 (45), 16834–16839. http://dx.doi.org/10.1073/pnas.0605296103.

Chocyk, A., Bobula, B., Dudys, D., Przyborowska, A., Majcher-Maslanka, I., Hess, G., Wedzony, K., 2013. Early-life stress affects the structural and functional plasticity of the medial prefrontal cortex in adolescent rats. Eur. J. Neurosci. 38 (1), 2089–2107. http://dx.doi.org/10.1111/ejn.12208.

Ciocchi, S., Passecker, J., Malagon-Vina, H., Mikus, N., Klausberger, T., 2015. Selective information routing by ventral hippocampal CA1 projection neurons. Science 348 (6234), 560–563. http://dx.doi.org/10.1126/science.aaa3245.

Clement, J.P., Aceti, M., Creson, T.K., Ozkan, E.D., Shi, Y., Reish, N.J., Almonte, A.G., Miller, B.H., Wiltgen, B.J., Miller, C.A., Xu, X., Rumbaugh, G., 2012. Pathogenic SYNGAP1 mutations impair cognitive development by disrupting maturation of

dendritic spine synapses. Cell 151 (4), 709–723. http://dx.doi.org/10.1016/j.cell.2012.08.045.
Dumitriu, D., Rodriguez, A., Morrison, J.H., 2011. High-throughput, detailed, cell-specific neuroanatomy of dendritic spines using microinjection and confocal microscopy. Nat. Protoc. 6 (9), 1391–1411. http://dx.doi.org/10.1038/nprot.2011.389.
Duncan, L.E., Pollastri, A.R., Smoller, J.W., 2014. Mind the gap: why many geneticists and psychological scientists have discrepant views about gene-environment interaction (GxE) research. Am. Psychol. 69 (3), 249–268. http://dx.doi.org/10.1037/a0036320.
Eagleson, K.L., Lane, C.J., McFadyen-Ketchum, L., Solak, S., Wu, H.H., Levitt, P., 2016. Distinct intracellular signaling mediates C-MET regulation of dendritic growth and synaptogenesis. Dev. Neurobiol. http://dx.doi.org/10.1002/dneu.22382.
Eagleson, K.L., Milner, T.A., Xie, Z., Levitt, P., 2013. Synaptic and extrasynaptic location of the receptor tyrosine kinase met during postnatal development in the mouse neocortex and hippocampus. J. Comp. Neurol. 521 (14), 3241–3259. http://dx.doi.org/10.1002/cne.23343.
Eiland, L., McEwen, B.S., 2012. Early life stress followed by subsequent adult chronic stress potentiates anxiety and blunts hippocampal structural remodeling. Hippocampus 22 (1), 82–91. http://dx.doi.org/10.1002/hipo.20862.
Fabricius, K., Wortwein, G., Pakkenberg, B., 2008. The impact of maternal separation on adult mouse behaviour and on the total neuron number in the mouse hippocampus. Brain Struct. Funct. 212 (5), 403–416. http://dx.doi.org/10.1007/s00429-007-0169-6.
Felix-Ortiz, A.C., Beyeler, A., Seo, C., Leppla, C.A., Wildes, C.P., Tye, K.M., 2013. BLA to vHPC inputs modulate anxiety-related behaviors. Neuron 79 (4), 658–664. http://dx.doi.org/10.1016/j.neuron.2013.06.016.
Felix-Ortiz, A.C., Tye, K.M., 2014. Amygdala inputs to the ventral hippocampus bidirectionally modulate social behavior. J. Neurosci. 34 (2), 586–595. http://dx.doi.org/10.1523/JNEUROSCI.4257-13.2014.
Francis, D.D., Meaney, M.J., 1999. Maternal care and the development of stress responses. Curr. Opin. Neurobiol. 9 (1), 128–134. http://dx.doi.org/10.1016/S0959-4388(99)80016-6.
Franklin, K.B.J., Paxinos, G., 2007. The Mouse Brain in Stereotaxic Coordinates, 3rd. ed. Academic Press.
Franklin, T.B., Linder, N., Russig, H., Thony, B., Mansuy, I.M., 2011. Influence of early stress on social abilities and serotonergic functions across generations in mice. PLoS One 6 (7), e21842. http://dx.doi.org/10.1371/journal.pone.0021842.
Graves, A.R., Moore, S.J., Bloss, E.B., Mensh, B.D., Kath, W.L., Spruston, N., 2012. Hippocampal pyramidal neurons comprise two distinct cell types that are countermodulated by metabotropic receptors. Neuron 76 (4), 776–789. http://dx.doi.org/10.1016/j.neuron.2012.09.036.
Green, J.G., McLaughlin, K.A., Berglund, P.A., Gruber, M.J., Sampson, N.A., Zaslavsky, A.M., Kessler, R.C., 2010. Childhood adversities and adult psychiatric disorders in the national comorbidity survey replication I: associations with first onset of DSM-IV disorders. Arch. Gen. Psychiatry 67 (2), 113–123. http://dx.doi.org/10.1001/archgenpsychiatry.2009.186.
Gutierrez, H., Dolcet, X., Tolcos, M., Davies, A., 2004. HGF regulates the development of cortical pyramidal dendrites. Development 131 (15), 3717–3726. http://dx.doi.org/10.1242/dev.01209.
Harrison, E.L., Jaehne, E.J., Jawahar, M.C., Corrigan, F., Baune, B.T., 2014. Maternal separation modifies behavioural and neuroendocrine responses to stress in CCR7 deficient mice. Behav. Brain Res. 263, 169–175. http://dx.doi.org/10.1016/j.bbr.2014.01.036.
Hedrick, A., Lee, Y., Wallace, G.L., Greenstein, D., Clasen, L., Giedd, J.N., Raznahan, A., 2012. Autism risk gene MET variation and cortical thickness in typically developing children and adolescents. Autism Res. 5 (6), 434–439. http://dx.doi.org/10.1002/aur.1256.
Henson, M.A., Larsen, R.S., Lawson, S.N., Perez-Otano, I., Nakanishi, N., Lipton, S.A., Philpot, B.D., 2012. Genetic deletion of NR3A accelerates glutamatergic synapse maturation. PLoS One 7 (8), e42327. http://dx.doi.org/10.1371/journal.pone.0042327.
Hettema, J.M., Neale, M.C., Kendler, K.S., 2001. A review and meta-analysis of the genetic epidemiology of anxiety disorders. Am. J. Psychiatry 158 (10), 1568–1578. http://dx.doi.org/10.1176/appi.ajp.158.10.1568.
Heuer, L., Braunschweig, D., Ashwood, P., Van de Water, J., Campbell, D.B., 2011. Association of a MET genetic variant with autism-associated maternal autoantibodies to fetal brain proteins and cytokine expression. Transl. Psychiatry 1, e48. http://dx.doi.org/10.1038/tp.2011.48.
Heun-Johnson, H., Levitt, P., 2016. Early-life stress paradigm transiently alters maternal behavior, dam-pup interactions, and offspring vocalizations in mice. Front. Behav. Neurosci. 10, 142. http://dx.doi.org/10.3389/fnbeh.2016.00142.
Huff, M.L., Emmons, E.B., Narayanan, N.S., LaLumiere, R.T., 2016. Basolateral amygdala projections to ventral hippocampus modulate the consolidation of footshock, but not contextual, learning in rats. Learn Mem. 23 (2), 51–60. http://dx.doi.org/10.1101/lm.039909.115.
Ivy, A.S., Brunson, K.L., Sandman, C., Baram, T.Z., 2008. Dysfunctional nurturing behavior in rat dams with limited access to nesting material: a clinically relevant model for early-life stress. Neuroscience 154 (3), 1132–1142. http://dx.doi.org/10.1016/j.neuroscience.2008.04.019.
Ivy, A.S., Rex, C.S., Chen, Y., Dube, C., Maras, P.M., Grigoriadis, D.E., Gall, C.M., Lynch, G., Baram, T.Z., 2010. Hippocampal dysfunction and cognitive impairments provoked by chronic early-life stress involve excessive activation of CRH receptors. J. Neurosci. 30 (39), 13005–13015. http://dx.doi.org/10.1523/JNEUROSCI.1784-10.2010.
Jackson, P.B., Boccuto, L., Skinner, C., Collins, J.S., Neri, G., Gurrieri, F., Schwartz, C.E., 2009. Further evidence that the rs1858830 C variant in the promoter region of the MET gene is associated with autistic disorder. Autism Res. 2 (4), 232–236. http://dx.doi.org/10.1002/aur.87.
Judson, M.C., Amaral, D.G., Levitt, P., 2011a. Conserved subcortical and divergent cortical expression of proteins encoded by orthologs of the autism risk gene MET. Cereb. Cortex 21 (7), 1613–1626. http://dx.doi.org/10.1093/cercor/bhq223.
Judson, M.C., Bergman, M.Y., Campbell, D.B., Eagleson, K.L., Levitt, P., 2009. Dynamic gene and protein expression patterns of the autism-associated met receptor tyrosine kinase in the developing mouse forebrain. J. Comp. Neurol. 513 (5), 511–531. http://dx.doi.org/10.1002/cne.21969.
Judson, M.C., Eagleson, K.L., Levitt, P., 2011b. A new synaptic player leading to autism risk: met receptor tyrosine kinase. J. Neurodev. Disord. 3 (3), 282–292. http://dx.doi.org/10.1007/s11689-011-9081-8.
Judson, M.C., Eagleson, K.L., Wang, L., Levitt, P., 2010. Evidence of cell-nonautonomous changes in dendrite and dendritic spine morphology in the met-signaling-deficient mouse forebrain. J. Comp. Neurol. 518 (21), 4463–4478. http://dx.doi.org/10.1002/cne.22467.
Kanatsou, S., Ter Horst, J.P., Harris, A.P., Seckl, J.R., Krugers, J., Joëls, M., 2016. Effects of mineralocorticoid receptor overexpression on anxiety and memory after early life stress in female mice. Front. Behav. Neurosci. http://dx.doi.org/10.3389/fnbeh.2015.00374.
Koe, A.S., Ashokan, A., Mitra, R., 2016. Short environmental enrichment in adulthood reverses anxiety and basolateral amygdala hypertrophy induced by maternal separation. Transl. Psychiatry 6, e729. http://dx.doi.org/10.1038/tp.2015.217.
Lang, A.J., Aarons, G.A., Gearity, J., Laffaye, C., Satz, L., Dresselhaus, T.R., Stein, M.B., 2008. Direct and indirect links between childhood maltreatment, posttraumatic stress disorder, and women's health. Behav. Med. 33 (4), 125–135. http://dx.doi.org/10.3200/BMED.33.4.125-136.
Lau, T., Bigio, B., Zelli, D., McEwen, B.S., Nasca, C., 2017. Stress-induced structural plasticity of medial amygdala stellate neurons and rapid prevention by a candidate antidepressant. Mol. Psychiatry 22 (2), 227–234. http://dx.doi.org/10.1038/mp.2016.68.
Levine, A., Worrell, T.R., Zimnisky, R., Schmauss, C., 2012. Early life stress triggers sustained changes in histone deacetylase expression and histone H4 modifications that alter responsiveness to adolescent antidepressant treatment. Neurobiol. Dis. 45 (1), 488–498. http://dx.doi.org/10.1016/j.nbd.2011.09.005.
Liao, X.M., Yang, X.D., Jia, J., Li, J.T., Xie, X.M., Su, Y.A., Schmidt, M.V., Si, T.M., Wang, X.D., 2014. Blockade of corticotropin-releasing hormone receptor 1 attenuates early-life stress-induced synaptic abnormalities in the neonatal hippocampus. Hippocampus 24 (5), 528–540. http://dx.doi.org/10.1002/hipo.22254.
Lim, C.S., Walikonis, R.S., 2008. Hepatocyte growth factor and c-Met promote dendritic maturation during hippocampal neuron differentiation via the Akt pathway. Cell Signal 20 (5), 825–835. http://dx.doi.org/10.1016/j.cellsig.2007.12.013.
Liu, R., Yang, X.D., Liao, X.M., Xie, X.M., Su, Y.A., Li, J.T., Wang, X.D., Si, T.M., 2016. Early postnatal stress suppresses the developmental trajectory of hippocampal pyramidal neurons: the role of CRHR1. Brain Struct. Funct. 221 (9), 4525–4536. http://dx.doi.org/10.1007/s00429-016-1182-4.
Maren, S., Anagnostaras, S.G., Fanselow, M.S., 1998. The startled seahorse: is the hippocampus necessary for contextual fear conditioning? Trends Cogn. Sci. 2 (2), 39–42. http://dx.doi.org/10.1016/S1364-6613(98)01123-1.
Maren, S., Fanselow, M.S., 1995. Synaptic plasticity in the basolateral amygdala induced by hippocampal formation stimulation in vivo. J. Neurosci. 15 (11), 7548–7564.
McDonald, A.J., Mott, D.D., 2017. Functional neuroanatomy of amygdalohippocampal interconnections and their role in learning and memory. J. Neurosci. Res. 95 (3), 797–820. http://dx.doi.org/10.1002/jnr.23709.
Mehta, M., Schmauss, C., 2011. Strain-specific cognitive deficits in adult mice exposed to early life stress. Behav. Neurosci. 125 (1), 29–36. http://dx.doi.org/10.1037/a0021952.
Monroy, E., Hernández-Torres, E., Flores, G., 2010. Maternal separation disrupts dendritic morphology of neurons in prefrontal cortex, hippocampus, and nucleus accumbens in male rat offspring. J. Chem. Neuroanat. 40 (2), 93–101. http://dx.doi.org/10.1016/j.jchemneu.2010.05.005.
Naninck, E.F., Hoeijmakers, L., Kakava-Georgiadou, N., Meesters, A., Lazic, S.E., Lucassen, P.J., Korosi, A., 2015. Chronic early life stress alters developmental and adult neurogenesis and impairs cognitive function in mice. Hippocampus 25 (3), 309–328. http://dx.doi.org/10.1002/hipo.22374.
Okaty, B.W., Freret, M.E., Rood, B.D., Brust, R.D., Hennessy, M.L., deBairos, D., Kim, J.C., Cook, M.N., Dymecki, S.M., 2015. Multi-scale molecular deconstruction of the serotonin neuron system. Neuron 88 (4), 774–791. http://dx.doi.org/10.1016/j.neuron.2015.10.007.
Okuyama, T., Kitamura, T., Roy, D.S., Itohara, S., Tonegawa, S., 2016. Ventral CA1 neurons store social memory. Science 353 (6307), 1536–1541. http://dx.doi.org/10.1126/science.aaf7003.
Padilla-Coreano, N., Bolkan, S.S., Pierce, G.M., Blackman, D.R., Hardin, W.D., Garcia-Garcia, A.L., Spellman, T.J., Gordon, J.A., 2016. Direct ventral hippocampal-prefrontal input is required for anxiety-related neural activity and behavior. Neuron 89 (4), 857–866. http://dx.doi.org/10.1016/j.neuron.2016.01.011.
Peng, Y., Lu, Z., Li, G., Piechowicz, M., Anderson, M., Uddin, Y., Wu, J., Qiu, S., 2016. The autism-associated MET receptor tyrosine kinase engages early neuronal growth mechanism and controls glutamatergic circuits development in the forebrain. Mol. Psychiatry 21 (7), 925–935. http://dx.doi.org/10.1038/mp.2015.182.
Qiu, S., Anderson, C.T., Levitt, P., Shepherd, G.M., 2011. Circuit-specific intracortical hyperconnectivity in mice with deletion of the autism-associated Met receptor tyrosine kinase. J. Neurosci. 31 (15), 5855–5864. http://dx.doi.org/10.1523/JNEUROSCI.6569-10.2011.
Qiu, S., Lu, Z., Levitt, P., 2014. MET receptor tyrosine kinase controls dendritic complexity, spine morphogenesis, and glutamatergic synapse maturation in the

hippocampus. J. Neurosci. 34 (49), 16166–16179. http://dx.doi.org/10.1523/JNEUROSCI.2580-14.2014.
Raineki, C., Cortes, M.R., Belnoue, L., Sullivan, R.M., 2012. Effects of early-life abuse differ across development: infant social behavior deficits are followed by adolescent depressive-like behaviors mediated by the amygdala. J. Neurosci. 32 (22), 7758–7765. http://dx.doi.org/10.1523/JNEUROSCI.5843-11.2012.
Raineki, C., Moriceau, S., Sullivan, R.M., 2010. Developing a neurobehavioral animal model of infant attachment to an abusive caregiver. Biol. Psychiatry 67 (12), 1137–1145. http://dx.doi.org/10.1016/j.biopsych.2009.12.019.
Raineki, C., Sarro, E., Rincon-Cortes, M., Perry, R., Boggs, J., Holman, C.J., Wilson, D.A., Sullivan, R.M., 2015. Paradoxical neurobehavioral rescue by memories of early-life abuse: the safety signal value of odors learned during abusive attachment. Neuropsychopharmacology 40 (4), 906–914. http://dx.doi.org/10.1038/npp.2014.266.
Rice, C.J., Sandman, C.A., Lenjavi, M.R., Baram, T.Z., 2008. A novel mouse model for acute and long-lasting consequences of early life stress. Endocrinology 149 (10), 4892–4900. http://dx.doi.org/10.1210/en.2008-0633.
Rodriguez, A., Ehlenberger, D.B., Hof, P.R., Wearne, S.L., 2006. Rayburst sampling, an algorithm for automated three-dimensional shape analysis from laser scanning microscopy images. Nat. Protoc. 1 (4), 2152–2161. http://dx.doi.org/10.1038/nprot.2006.313.
Romano-Lopez, Q.F., Mendez-Diaz, M.D., Garcia, F.G.D., Regalado-Santiago, C.D., Ruiz Contreras, A.E.D., Prospero-Garcia, O.D., 2015. Maternal separation and early stress cause long-lasting effects on dopaminergic and endocannabinergic systems and alters dendritic morphology in the nucleus accumbens and frontal cortex in rats. Dev. Neurobiol. http://dx.doi.org/10.1002/dneu.22361.
Rudie, J.D., Hernandez, L.M., Brown, J.A., Beck-Pancer, D., Colich, N.L., Gorrindo, P., Thompson, P.M., Geschwind, D.H., Bookheimer, S.Y., Levitt, P., Dapretto, M., 2012. Autism-associated promoter variant in MET impacts functional and structural brain networks. Neuron 75 (5), 904–915. http://dx.doi.org/10.1016/j.neuron.2012.07.010.
Sachs, B.D., Rodriguiz, R.M., Siesser, W.B., Kenan, A., Royer, E.L., Jacobsen, J.P., Wetsel, W.C., Caron, M.G., 2013. The effects of brain serotonin deficiency on behavioural disinhibition and anxiety-like behaviour following mild early life stress. Int. J. Neuropsychopharmacol. 16 (9), 2081–2094. http://dx.doi.org/10.1017/S1461145713000321.
Santarelli, S., Lesuis, S.L., Wang, X.D., Wagner, K.V., Hartmann, J., Labermaier, C., Scharf, S.H., Muller, M.B., Holsboer, F., Schmidt, M.V., 2014. Evidence supporting the match/mismatch hypothesis of psychiatric disorders. Eur. Neuropsychopharmacol. 24 (6), 907–918. http://dx.doi.org/10.1016/j.euroneuro.2014.02.002.
Savignac, H.M., Dinan, T.G., Cryan, J.F., 2011. Resistance to early-life stress in mice: effects of genetic background and stress duration. Front. Behav. Neurosci. 5, 13. http://dx.doi.org/10.3389/fnbeh.2011.00013.
Sharma, S., Powers, A., Bradley, B., Ressler, K.J., 2015. Gene x environment determinants of stress- and anxiety-related disorders. Annu. Rev. Psychol. 67, 239–261. http://dx.doi.org/10.1146/annurev-psych-122414-033408.
Sholl, D.A., 1953. Dendritic organization in the neurons of the visual and motor cortices of the cat. J. Anat. 87 (4), 387–406.
Smith, D.M., Bulkin, D.A., 2014. The form and function of hippocampal context representations. Neurosci. Biobehav Rev. 40, 52–61. http://dx.doi.org/10.1016/j.neubiorev.2014.01.005.
Stein, M.B., Jang, K.L., Taylor, S., Vernon, P.A., Livesley, W.J., 2002. Genetic and environmental influences on trauma exposure and posttraumatic stress disorder symptoms: a twin study. Am. J. Psychiatry 159 (10), 1675–1681. http://dx.doi.org/10.1176/appi.ajp.159.10.1675.
Sullivan, P.F., Neale, M.C., Kendler, K.S., 2000. Genetic epidemiology of major depression: review and meta-analysis. Am. J. Psychiatry 157 (10), 1552–1562. http://dx.doi.org/10.1176/appi.ajp.157.10.1552.
Thompson, B.L., Levitt, P., 2015. Complete or partial reduction of the *Met* receptor tyrosine kinase in distinct circuits differentially impacts mouse behavior. J. Neurodev. Disord. 7, 35. http://dx.doi.org/10.1186/s11689-015-9131-8.
Toya, S., Takatsuru, Y., Kokubo, M., Amano, I., Shimokawa, N., Koibuchi, N., 2014. Early-life-stress affects the homeostasis of glutamatergic synapses. Eur. J. Neurosci. 40 (11), 3627–3634. http://dx.doi.org/10.1111/ejn.12728.
Tsuda, M.C., Ogawa, S., 2012. Long-lasting consequences of neonatal maternal separation on social behaviors in ovariectomized female mice. PLoS One 7 (3), e33028. http://dx.doi.org/10.1371/journal.pone.0033028.
Tsuda, M.C., Yamaguchi, N., Nakata, M., Ogawa, S., 2014. Modification of female and male social behaviors in estrogen receptor beta knockout mice by neonatal maternal separation. Front. Neurosci. 8, 274. http://dx.doi.org/10.3389/fnins.2014.00274.
Tsuda, M.C., Yamaguchi, N., Ogawa, S., 2011. Early life stress disrupts peripubertal development of aggression in male mice. Neuroreport 22 (6), 259–263. http://dx.doi.org/10.1097/WNR.0b013e328344495a.
van der Kooij, M.A., Grosse, J., Zanoletti, O., Papilloud, A., Sandi, C., 2015. The effects of stress during early postnatal periods on behavior and hippocampal neuroplasticity markers in adult male mice. Neuroscience 311, 508–518. http://dx.doi.org/10.1016/j.neuroscience.2015.10.058.
van Heerden, J.H., Russell, V., Korff, A., Stein, D.J., Illing, N., 2010. Evaluating the behavioural consequences of early maternal separation in adult C57BL/6 mice; the importance of time. Behav. Brain Res. 207 (2), 332–342. http://dx.doi.org/10.1016/j.bbr.2009.10.015.
Veenema, A.H., Bredewold, R., Neumann, I.D., 2007. Opposite effects of maternal separation on intermale and maternal aggression in C57BL/6 mice: link to hypothalamic vasopressin and oxytocin immunoreactivity. Psychoneuroendocrinology 32 (5), 437–450. http://dx.doi.org/10.1016/j.psyneuen.2007.02.008.
Venerosi, A., Cirulli, F., Capone, F., Alleva, E., 2003. Prolonged perinatal AZT administration and early maternal separation: effects on social and emotional behaviour of periadolescent mice. Pharmacol. Biochem. Behav. 74 (3), 671–681. http://dx.doi.org/10.1016/S0091-3057(02)01068-7.
Voineagu, I., Wang, X., Johnston, P., Lowe, J.K., Tian, Y., Horvath, S., Mill, J., Cantor, R.M., Blencowe, B.J., Geschwind, D.H., 2011. Transcriptomic analysis of autistic brain reveals convergent molecular pathology. Nature 474 (7351), 380–384. http://dx.doi.org/10.1038/nature10110.
Volk, H.E., Kerin, T., Lurmann, F., Hertz-Picciotto, I., McConnell, R., Campbell, D.B., 2014. Autism spectrum disorder: interaction of air pollution with the MET receptor tyrosine kinase gene. Epidemiology 25 (1), 44–47. http://dx.doi.org/10.1097/EDE.0000000000000030.
Wang, L., Jiao, J., Dulawa, S.C., 2011a. Infant maternal separation impairs adult cognitive performance in BALB/cJ mice. Psychopharmacol. Berl. 216 (2), 207–218. http://dx.doi.org/10.1007/s00213-011-2209-4.
Wang, X.D., Labermaier, C., Holsboer, F., Wurst, W., Deussing, J.M., Muller, M.B., Schmidt, M.V., 2012. Early-life stress-induced anxiety-related behavior in adult mice partially requires forebrain corticotropin-releasing hormone receptor 1. Eur. J. Neurosci. 36 (3), 2360–2367. http://dx.doi.org/10.1111/j.1460-9568.2012.08148.x.
Wang, X.D., Rammes, G., Kraev, I., Wolf, M., Liebl, C., Scharf, S.H., Rice, C.J., Wurst, W., Holsboer, F., Deussing, J.M., Baram, T.Z., Stewart, M.G., Muller, M.B., Schmidt, M.V., 2011b. Forebrain CRF(1) modulates early-life stress-programmed cognitive deficits. J. Neurosci. 31 (38), 13625–13634. http://dx.doi.org/10.1523/JNEUROSCI.2259-11.2011.
Wang, X.D., Su, Y.A., Wagner, K.V., Avrabos, C., Scharf, S.H., Hartmann, J., Wolf, M., Liebl, C., Kuhne, C., Wurst, W., Holsboer, F., Eder, M., Deussing, J.M., Muller, M.B., Schmidt, M.V., 2013. Nectin-3 links CRHR1 signaling to stress-induced memory deficits and spine loss. Nat. Neurosci. 16 (6), 706–713. http://dx.doi.org/10.1038/nn.3395.
Wearne, S.L., Rodriguez, A., Ehlenberger, D.B., Rocher, A.B., Henderson, S.C., Hof, P.R., 2005. New techniques for imaging, digitization and analysis of three-dimensional neural morphology on multiple scales. Neuroscience 136 (3), 661–680. http://dx.doi.org/10.1016/j.neuroscience.2005.05.053.
Widom, C.S., 1999. Posttraumatic stress disorder in abused and neglected children grown up. Am. J. Psychiatry 156 (8), 1223–1229. http://dx.doi.org/10.1176/ajp.156.8.1223.
Xie, L., Korkmaz, K.S., Braun, K., Bock, J., 2013. Early life stress-induced histone acetylations correlate with activation of the synaptic plasticity genes Arc and Egr1 in the mouse hippocampus. J. Neurochem. 125 (3), 457–464. http://dx.doi.org/10.1111/jnc.12210.
Xu, C., Krabbe, S., Grundemann, J., Botta, P., Fadok, J.P., Osakada, F., Saur, D., Grewe, B.F., Schnitzer, M.J., Callaway, E.M., Luthi, A., 2016. Distinct hippocampal pathways mediate dissociable roles of context in memory retrieval. Cell 167 (4). http://dx.doi.org/10.1016/j.cell.2016.09.051. 961–972 e916.
Yang, X.D., Liao, X.M., Uribe-Marino, A., Liu, R., Xie, X.M., Jia, J., Su, Y.A., Li, J.T., Schmidt, M.V., Wang, X.D., Si, T.M., 2015. Stress during a critical postnatal period induces region-specific structural abnormalities and dysfunction of the prefrontal cortex via CRF1. Neuropsychopharmacology 40 (5), 1203–1215. http://dx.doi.org/10.1038/npp.2014.304.
Zoicas, I., Neumann, I.D., 2016. Maternal separation facilitates extinction of social fear in adult male mice. Behav. Brain Res. 297, 323–328. http://dx.doi.org/10.1016/j.bbr.2015.10.034.